

# UC Santa Barbara

## UC Santa Barbara Previously Published Works

### Title

A "Traceless" Directing Group Enables Catalytic S N 2 Glycosylation toward 1,2-cis-Glycopyranosides

### Permalink

<https://escholarship.org/uc/item/0qf8k4t7>

### Journal

Journal of the American Chemical Society, 143(31)

### ISSN

0002-7863

### Authors

Ma, Xu  
Zheng, Zhitong  
Fu, Yue  
[et al.](#)

### Publication Date

2021-08-11

### DOI

10.1021/jacs.1c04584

Peer reviewed



Published in final edited form as:

*J Am Chem Soc.* 2021 August 11; 143(31): 11908–11913. doi:10.1021/jacs.1c04584.

## A “Traceless” Directing Group Enables Catalytic $S_N2$ Glycosylation toward 1,2-*cis*-Glycopyranosides

**Xu Ma**<sup>§</sup>,

Department of Chemistry & Biochemistry, University of California, Santa Barbara, California 93106, United States

**Zhitong Zheng**<sup>§</sup>,

Department of Chemistry & Biochemistry, University of California, Santa Barbara, California 93106, United States

**Yue Fu**<sup>§</sup>,

Department of Chemistry, University of Pittsburgh, Pittsburgh, Pennsylvania 15260, United States

**Xijun Zhu,**

Department of Chemistry & Biochemistry, University of California, Santa Barbara, California 93106, United States

**Peng Liu,**

Department of Chemistry, University of Pittsburgh, Pittsburgh, Pennsylvania 15260, United States

**Liming Zhang**

Department of Chemistry & Biochemistry, University of California, Santa Barbara, California 93106, United States

### Abstract

Generally applicable and stereoselective formation of 1,2-*cis*-glycopyranosidic linkage remains a long sought after yet unmet goal in carbohydrate chemistry. This work advances a strategy to this challenge via stereoinversion at the anomeric position of 1,2-*trans* glycosyl ester donors. This  $S_N2$  glycosylation is enabled under gold catalysis by an oxazole-based directing group optimally tethered to a leaving group and achieved under mild catalytic conditions, in mostly excellent yields, and with good to outstanding selectivities. The strategy is also applied to the synthesis of oligosaccharides.

---

**Corresponding Authors:** Peng Liu – pengliu@pitt.edu, Liming Zhang – zhang@chem.ucsb.edu.

<sup>§</sup>Author Contributions

X.M., Z.Z., and Y.F. contributed equally to this work.

The authors declare no competing financial interest.

#### ASSOCIATED CONTENT

##### Supporting Information

The Supporting Information is available free of charge at <https://pubs.acs.org/doi/10.1021/jacs.1c04584>.

Experimental procedures and characterization data, computational study results, Cartesian coordinates, and spectral data (PDF)

Complete contact information is available at: <https://pubs.acs.org/doi/10.1021/jacs.1c04584>

The main challenge arising from the construction of glycosidic bonds in oligosaccharide synthesis<sup>1,2</sup> is how to control the anomeric configuration formed from a diverse array of glycosyl donors and acceptors. Remarkable advances in stereoselective glycosylation reactions have been achieved and especially in the context of the formation of 1,2-*trans* glycosidic bonds via neighboring group participation (Figure 1A). In contrast, the formation of 1,2-*cis* glycosidic bonds remains challenging, and a much-needed strategy that is generally applicable to every sugar donor type has yet to be developed. Some innovative methods<sup>3–6</sup> partially addressing this challenge are shown in Figure 1B. Due to the need to install a special directing group or protecting group (PG) on the sugar ring, they suffer from limited scope and/or complicated donor synthesis. Moreover, such groups may complicate subsequent glycosylation or requiring additional PG manipulation. Alternative strategies for the synthesis of 1,2-*cis*-glycosides relying on solvent effects<sup>7,8</sup> or halide ion catalysis<sup>9</sup> are also limited by applicable scope.

We envisioned an S<sub>N</sub>2 glycosylation strategy that features a basic group installed on the glycosyl leaving group (LG) and facilitating acceptor attack (Figure 1C). This strategy allows simultaneous activation of donor and acceptor and mimics glycosyl hydrolases/transferases<sup>10</sup> and would conceptually accommodate any glycosyl donors, regardless of their configurations and protecting group patterns. We term this as directing-group-on-leaving-group (DGLG). Upon glycosylation, this directing group departs along with the leaving group and hence can be considered “traceless” in the glycoside product. This design necessitates S<sub>N</sub>2 glycosylation in order to harness the directing effect. By using a 1,2-*trans*-glycosyl donor, this strategy would lead to general access to the challenging 1,2-*cis*-glycosides. Notably, other remarkable catalytic strategies of simultaneous donor and acceptor activation for S<sub>N</sub>2-type glycosylation have been reported,<sup>5,11–14</sup> including Schmidt’s acid–base catalysis<sup>11</sup> and Jacobsen’s macrocyclic bithiourea-catalyzed glycosylation.<sup>12–14</sup>

In practice, we engineered the LG based on the *ortho*-alkynylbenzoates used in Yu’s glycosylation chemistry.<sup>15</sup> As shown in Scheme 1A, in the designed donor **1**, the *ortho* C–C triple bond is terminated by an alkynylcyclopropyl group, which features a mildly basic oxazole ring. It is anticipated that its gold-promoted cyclization would deliver isochromenylium intermediate **A**,<sup>16</sup> which has its side arm oxazole ring positioned to direct an alcohol acceptor to attack at the backend of the activated anomeric C–O bond. Such delivery of the acceptor would afford glycoside **2** with the inverted configuration at the anomeric carbon and hence realize the desired S<sub>N</sub>2 glycosylation.

The designed donors can be prepared straightforwardly via two consecutive Sonogashira couplings (see the Supporting Information for details), and some representative ones are shown in Scheme 1B. Table 1 outlines the condition optimization for the synthesis of methyl D-glucopyranosyl-(1 → 6)-*α*-D-glucopyranoside **5a** from the *β*-D-glucopyranosyl donors (Scheme 1B) and the acceptor methyl *α*-D-glucopyranoside **4a**. To our delight, with **D1** as the donor, **5a** was obtained with a respectable *α/β* ratio of 11:1 in the presence of 20 mol % PPh<sub>3</sub>AuNTf<sub>2</sub> in CH<sub>2</sub>Cl<sub>2</sub> (DCM) at –35 °C (entry 1). In comparison, donor **D2** devoid of oxazole led to little stereoselectivity (entry 2), revealing the critical role of the basic heterocycle in enabling anomeric configuration inversion. By increasing the gold catalyst

loading to 0.5 and 1.0 equiv, the  $\alpha/\beta$  ratio was lowered to 2.8:1 (entry 3) and 1.5:1 (entry 4), respectively. These results are consistent with the directing role played by the oxazole nitrogen as the cationic gold(I) increasingly binds to it and hence diminishes its designed function. This detrimental binding of oxazole to Au(I) is even more pronounced with donor **D3**, of which the oxazole is devoid of substitution at its C2 position and hence presents an unhindered ring nitrogen for coordination. In this case, the gold catalyst appeared to be largely sequestered (entry 5). Upon further donor and conditions optimization, we discovered that donor **D4** bearing two methoxy groups on its benzoate permits a faster reaction while maintaining similar  $\alpha$  selectivity (entry 6). With  $\text{IMesAu}^+ \text{BARF}^-$  generated from  $\text{IMesAuCl}/[\text{Ag}(\text{MeCN})_2]^+ \text{BARF}^-$  as the catalyst in 5 mol %, the reaction was sluggish at 0 °C. With 62% conversion after 16 h, the  $\alpha/\beta$  selectivity was, however, improved to >20:1 (entry 7). Changing the reaction solvent from DCM to  $\text{PhCF}_3$  led to near quantitative yield while maintaining excellent  $\alpha$  selectivity (entry 8). Lowering the reaction temperature led to an even better selectivity but at the cost of conversion (entry 9). The solvent effect, as evident from entries 7 and 8, was further examined. We discovered that isochromen-1-one byproduct **3** ( $R' = 3,4\text{-(MeO)}_2$ ) is crystalline and has significantly higher solubility in DCM (>0.02 M at -15 °C) Table 1. Reaction Discovery and Optimization than in  $\text{PhCF}_3$  (~0.0056 M at -15 °C). It is reasoned that the slower reaction rate in DCM is partly due to the coordination of Au(I) by oxazole nitrogen of **3**. In contrast, in  $\text{PhCF}_3$ , most of **3** precipitates out from the reaction. To this end, with a mixture of  $\text{PhCF}_3$  and even less dissolving cyclohexane ( $v/v = 4:1$ ) and at an increased concentration (0.08 M), the reaction was substantially accelerated and proceeded to completion in 15 h at -15 °C (entry 10). The reaction was again quantitative in yield and highly  $\alpha$ -selective. In comparison, under these optimized conditions, **D2** again resulted in a poor  $\alpha/\beta$  ratio of 3.1/1 (entry 11).

The optimized conditions (i.e., Table 1, entry 10) were applied to a range of acceptors using **D4** as the donor. As shown in Figure 2, chiral alcohols like (*R*)-1-phenylethanol and L-menthol proceed with excellent yields and nearly exclusive  $\alpha$  selectivity (**5b** and **5c**). L-Serine esters and cholesterol were running in different solvents due to their poor solubility in the mixed solvent system, but the yields and  $\alpha$  selectivities remained high (**5d** and **5e**). The reaction of the galactopyranose-based primary alcohol acceptor proceeded in 90% yield and with >30:1  $\alpha/\beta$  ratios (**5f**). With methyl groups replacing the benzyl groups in **D4**, the selectivity was diminished to 13.5:1 (**5g**). We attribute this to the fact that methyl is less inductively electron-withdrawing than benzyl; consequently, the methylated donor has a higher tendency of participating in the  $S_N1$  pathway. We then examined tri-*O*-benzyl-D-glucopyranoside acceptors with a secondary hydroxy group at 2-, 3-, or 4-position (**5h–5j**). While the yields are all high, the  $\alpha/\beta$  selectivity ranges from >20:1 for the 1 → 2 linkage to 11:1 for the 1 → 4 linkage and 6:1 for the 1 → 3 linkage. We also prepared the 4-*t*-butylbenzyl counterpart of donor **D4**, which shall be more soluble in nonpolar solvents, but the improvement was marginal (**5k**). The D-glucofuranose and L-rhamnopyranose-derived acceptors also reacted well, exhibiting excellent yields and selectivities (**5l** and **5m**), while the reaction of methyl  $\alpha$ -2,3,6-tri-*O*-benzylgalactopyranoside exhibited a respectable 11:1 preference for the  $\alpha$ -glycosidic linkage (**5n**). With readily removable acetyl replacing the *O*-6-benzyl group in **D4**, generally higher selectivities were observed (**5o–5q**). This gold catalysis also tolerates a thioglycoside as the acceptor (**5q**). In addition, modifying **D4** by

replacing the 4-*O*-benzyl group with acetyl, by installing 4,6-*O*-benzylidene, or by oxidizing it into methyl glucuronate was inconsequential, as the product from reacting with **1a** (i.e., **5r**, **5s**, or **5t**, respectively) was obtained in an excellent yield and with high  $\alpha$  selectivity.

We then applied this design to the synthesis of other 1,2-*cis*-pyranosides (Figure 3). The reaction of the corresponding  $\beta$ -D-galactopyranosyl donor with a primary or secondary alcohol donor also exhibited excellent  $\alpha$  selectivity, affording 1,2-*cis*-galactosides **5u** or **5v** in excellent yield (Figure 3A). The reaction of the xylopyranosyl donor was also highly  $\alpha$ -selective and efficient (Figure 3B). We then explored this  $S_N2$  glycosylation using  $\alpha$ -mannosyl donors. As shown in Figure 3C, only a moderate inversion of the anomeric configuration was detected in the case of **5x** when a tetra-*O*-benzylated version was employed. This result suggests that this DGLG strategy may be of limited utility for the synthesis of 1,2-*cis*-rhamnosides. To our delight, with a 4,6-benzylidene-protected  $\alpha$ -mannosyl donor,<sup>17</sup> the reactions exhibited exclusive  $S_N2$  characteristics regardless of the nature of the acceptor, and both **5y** and **5z** were formed in only  $\beta$ -forms. In comparison, with a donor without the oxazole group, **5y** was formed with an  $\alpha/\beta$  ratio of 1:13, and **5z** was formed in a literature report<sup>18</sup> of 1:12, revealing the beneficial directing effect in addition to the inherent selectivity. A reported drawback<sup>19</sup> of employing 4,6-*O*-benzylidene-mannosyl donors<sup>20</sup> is the substantially diminished selectivities caused by adverse steric buttressing of bulky O3 groups. Despite subsequent improvements via using sterically minimal propargyl as the O2 protecting group<sup>21</sup> or employing Yu's  $\alpha$ -alkynylbenzoate system,<sup>18</sup> the issue remains with bulky acceptors. For example, mannoside **5ab** containing a bulky 3'-*O*-TBS group formed from the sterically demanding secondary glucoside acceptor exhibited 7:1  $\beta/\alpha$  ratios. Using our strategy, **5ab** was formed with an improved  $\beta/\alpha$  ratio of 13:1. Remarkably, the reaction was run at ambient temperature, which is advantageous over literature cryogenic conditions (e.g.,  $-20\text{ }^\circ\text{C}$ <sup>18</sup> and  $-78\text{ }^\circ\text{C}$ <sup>21</sup>). This strategy was also successfully applied to the synthesis of **5aa**.

To demonstrate the utility of this strategy, we applied it to oligosaccharide synthesis. As shown in Scheme 2A, using methyl 2,3,4-tri-*O*-benzyl-D-glucopyranoside (**4a**) as the initial acceptor and the 6-acetate analog of **D4** (i.e., **D5**) as the donor, an iterative process consisting of glycosylation and basic hydrolysis delivered protected isomaltotetraose **6c** in 78% overall yield and excellent  $\alpha$  selectivities after three iterations. Alternatively, related maltotriose derivative **6d** can be accessed in one step from  $\alpha$ -maltose-derived donor **D6** in 88% yield and with good  $\alpha$  selectivity (Scheme 2B). In addition, as shown in Scheme 2C, we examined chemoselectivity by employing methyl 2,3-di-*O*-benzyl- $\alpha$ -D-glucopyranoside as the acceptor. Its reaction with **D4** indeed selectively glycosylated the more accessible 6-OH group to afford disaccharide **5ac** with excellent  $\alpha$  selectivity and in 92% yield. It was then reacted with mannose-derived donor **D7** to afford branched trisaccharide **6e** in 89% yield and with an  $\beta/\alpha$  ratio of >20:1. This two-step sequence was also run successfully in one pot.

To offer insight into the high levels of stereospecificity in the formation of 1,2-*cis* glycosidic bonds, we performed density functional theory (DFT) calculations to study the  $S_N1$  and  $S_N2$  pathways of the glycosylation of *O*-methylated analog of **D4** using MeOH as a model acceptor (Figure 4). The overall catalytic cycle (Figure S3) involves a facile Au(I)-catalyzed

cyclization of the *ortho*-alkynylbenzoate to form isochromenylium intermediate **7** with the twisted-boat conformation, which is 2.2 kcal/mol more stable than its chair conformation, **7a**, followed by a rate- and stereoselectivity-determining glycosylation step (Figure 4A). Glycosylation via the concerted  $S_N2$ -transition state (**TS2**) requires lower activation free energy than the leaving group dissociation (**TS1**) in the unimolecular  $S_N1$  pathway ( $G^\ddagger = 14.1$  and 16.8 kcal/mol, respectively).<sup>22</sup> These results suggest that the stereospecific  $S_N2$  reaction with the  $\beta$ -donor is faster than the formation of oxocarbenium ion in an  $S_N1$ -type process. To support this finding experimentally, the reaction of the per-methylated counterpart of **D4** with MeOH under the computed reaction conditions (i.e., Table 1, entry 9) yielded permethylated glucose **9** with  $\alpha/\beta > 50:1$ .

We then analyzed factors that promote  $S_N2$ -like transition state **TS2** (Figure 4B). **TS2** features a loose structure with relatively long  $C^1-O^{LG}$  and  $C^1-O^{Nu}$  distances (2.41 and 2.42 Å, respectively), which alleviate the 1,2-*cis* steric repulsion between  $C^2-OMe$  and the alcohol acceptor. The isochromenylium leaving group (LG) requires a relatively small distortion energy ( $E_{dist} = 9.7$  kcal/mol with respect to the dissociated leaving group and  $-2.9$  kcal/mol with respect to the LG in **7**) to orient the oxazole ring in the side arm to form a strong hydrogen bond with the alcohol acceptor ( $d(N-H) = 1.83$  Å). In addition, the isochromenylium ring is oriented perpendicular to the C6 oxygen lone pair. This geometry enables stabilizing lone pair/ $\pi$  interactions with the positively charged isochromenylium ring [see Figure S5 for the NCI (noncovalent interaction) plot visualization of the stabilizing interactions]. Finally, the lone pair/ $\pi$  interactions between the C6 oxygen and the isochromenylium promote the pyranose ring in the ground state of **7** to adopt a twisted-boat conformation, which minimizes the distortion of the pyranose ring to achieve the half-chair conformation ( ${}^4H_3$ ) in the  $S_N2$  transition state.

In conclusion, a gold-catalyzed  $S_N2$  glycosylation is developed to achieve access to challenging 1,2-*cis*-glycosidic linkages. This chemistry is enabled by a unique directing-group-on-leaving-group strategy, in which a “traceless” basic oxazole moiety is appended to the anomeric leaving group and engineered to direct the back-end attack at the anomeric center by a glycosyl acceptor. Under exceptionally mild conditions, the reactions exhibit mostly excellent yields and good to outstanding 1,2-*cis* selectivities. Notably, sterically demanding secondary glycosyl acceptors are readily allowed. The utilities of this strategy in oligosaccharide synthesis are successfully demonstrated.

## Supplementary Material

Refer to Web version on PubMed Central for supplementary material.

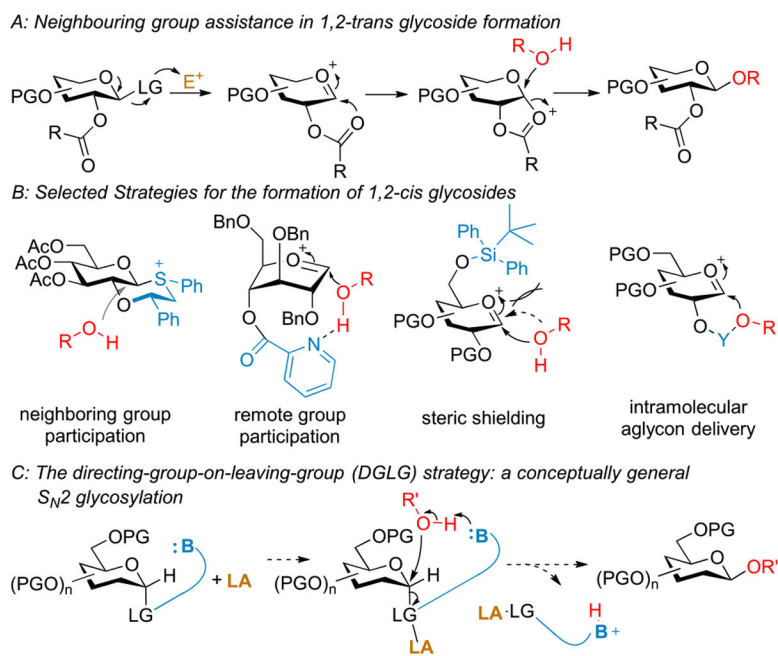
## ACKNOWLEDGMENTS

L.Z. thanks NIH glycoscience common fund 1U01GM125289 for financial support and NSF MRI-1920299 for the purchase of NMR instruments. P. L. thanks NIH R35GM128779 for financial support.

## REFERENCES

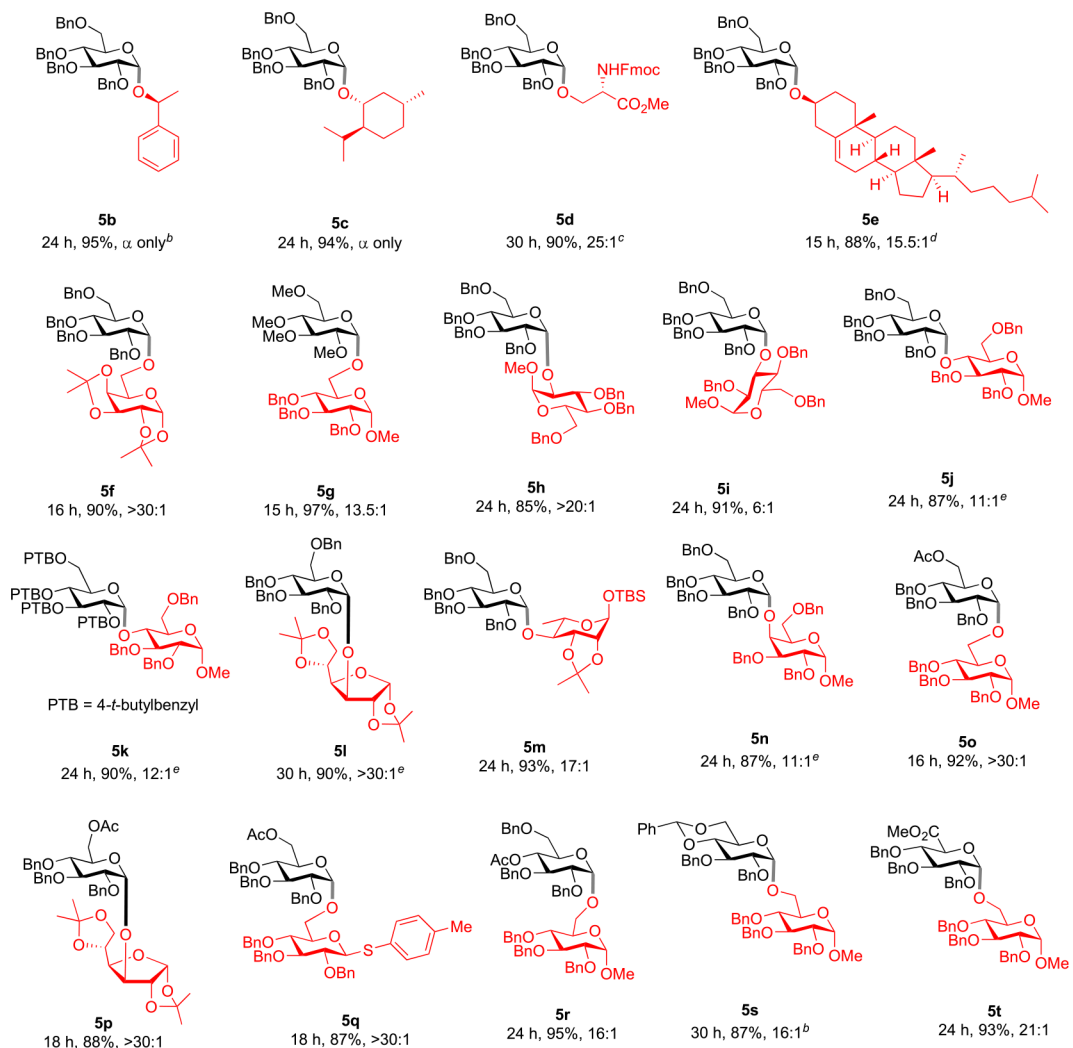
- (1). Fraser-Reid BO; Tatsuta K; Thiem J Glycoscience Chemistry and Chemical Biology, 2nd ed.; Springer-Verlag Berlin Heidelberg: Berlin, Heidelberg, 2008.

- (2). Werz DB; Vidal S Modern Synthetic Methods in Carbohydrate Chemistry: From Monosaccharides to Complex Glycoconjugates; Wiley-VCH Verlag GmbH & Co. KGaA, 2014.
- (3). Demchenko AV 1, 2-cis O-Glycosylation: methods, strategies, principles. *Curr. Org. Chem* 2003, 7, 35–79.
- (4). Nigudkar SS; Demchenko AV Stereocontrolled 1,2-cis glycosylation as the driving force of progress in synthetic carbohydrate chemistry. *Chem. Sci* 2015, 6, 2687–2704. [PubMed: 26078847]
- (5). Tanaka M; Nakagawa A; Nishi N; Iijima K; Sawa R; Takahashi D; Toshima K Boronic-Acid-Catalyzed Regioselective and 1,2-cis-Stereoselective Glycosylation of Unprotected Sugar Acceptors via S<sub>N</sub>i-Type Mechanism. *J. Am. Chem. Soc* 2018, 140, 3644–3651. [PubMed: 29457892]
- (6). Nguyen HM; Yu F; Li J; DeMent PM; Tu Y-J; Schlegel HB Phenanthroline-Catalyzed Stereoretentive Glycosylations. *Angew. Chem., Int. Ed* 2019, 58, 6957–6961.
- (7). Demchenko A; Stauch T; Boons G-J Solvent and Other Effects on the Stereoselectivity of Thioglycoside Glycosidations. *Synlett* 1997, 1997, 818–820.
- (8). Lu S-R; Lai Y-H; Chen J-H; Liu C-Y; Mong K-KT Dimethylformamide: An Unusual Glycosylation Modulator. *Angew. Chem., Int. Ed* 2011, 50, 7315–7320.
- (9). Lemieux RU; Hendriks KB; Stick RV; James K Halide ion catalyzed glycosidation reactions. Syntheses of  $\alpha$ -linked disaccharides. *J. Am. Chem. Soc* 1975, 97, 4056–4062.
- (10). Withers SG Mechanisms of glycosyl transferases and hydrolases. *Carbohydr. Polym* 2001, 44, 325–337.
- (11). Peng P; Schmidt RR Acid–Base Catalysis in Glycosidations: A Nature Derived Alternative to the Generally Employed Methodology. *Acc. Chem. Res* 2017, 50, 1171–1183. [PubMed: 28440624]
- (12). Park Y; Harper KC; Kuhl N; Kwan EE; Liu RY; Jacobsen EN Macrocyclic bis-thioureas catalyze stereospecific glycosylation reactions. *Science* 2017, 355, 162–166. [PubMed: 28082586]
- (13). Levi SM; Li Q; Rötheli AR; Jacobsen EN Catalytic activation of glycosyl phosphates for stereoselective coupling reactions. *Proc. Natl. Acad. Sci. U. S. A* 2019, 116, 35–39. [PubMed: 30559190]
- (14). Mayfield AB; Metternich JB; Trotta AH; Jacobsen EN Stereospecific Furanosylations Catalyzed by Bis-thiourea Hydrogen-Bond Donors. *J. Am. Chem. Soc* 2020, 142, 4061–4069. [PubMed: 32013410]
- (15). Yu B Gold(I)-Catalyzed Glycosylation with Glycosyl *o*-Alkynylbenzoates as Donors. *Acc. Chem. Res* 2018, 51, 507–516. [PubMed: 29297680]
- (16). Zhu Y; Yu B Characterization of the Isochromen-4-yl-gold(I) Intermediate in the Gold(I)-Catalyzed Glycosidation of Glycosyl *ortho*-Alkynylbenzoates and Enhancement of the Catalytic Efficiency Thereof. *Angew. Chem., Int. Ed* 2011, 50, 8329–8332.
- (17). Crich D; Sun S Formation of  $\beta$ -mannopyranosides of primary alcohols using the sulfoxide method. *J. Org. Chem* 1996, 61, 4506–4507. [PubMed: 11667369]
- (18). Zhu Y; Yu B Highly Stereoselective  $\beta$ -Mannopyranosylation via the 1- $\alpha$ -Glycosyloxy-isochromenylium-4-gold(I) Intermediates. *Chem. - Eur. J* 2015, 21, 8771–8780. [PubMed: 25899008]
- (19). Crich D; Dudkin V An unusual example of steric buttressing in glycosylation. *Tetrahedron Lett* 2000, 41, 5643–5646.
- (20). Crich D Chemistry of Glycosyl Triflates: Synthesis of  $\beta$ -Mannopyranosides. *J. Carbohydr. Chem* 2002, 21, 663–686.
- (21). Crich D; Jayalath P; Hutton TK Enhanced Diastereoselectivity in  $\beta$ -Mannopyranosylation through the Use of Sterically Minimal Propargyl Ether Protecting Groups. *J. Org. Chem* 2006, 71, 3064–3070. [PubMed: 16599600]
- (22). The computed activation free energies of the S<sub>N</sub>2 and S<sub>N</sub>1 pathways may be affected by the weakly coordinating counterion and the method for entropy calculations. See the Supporting Information for detailed discussions on the counterion and entropy effects.

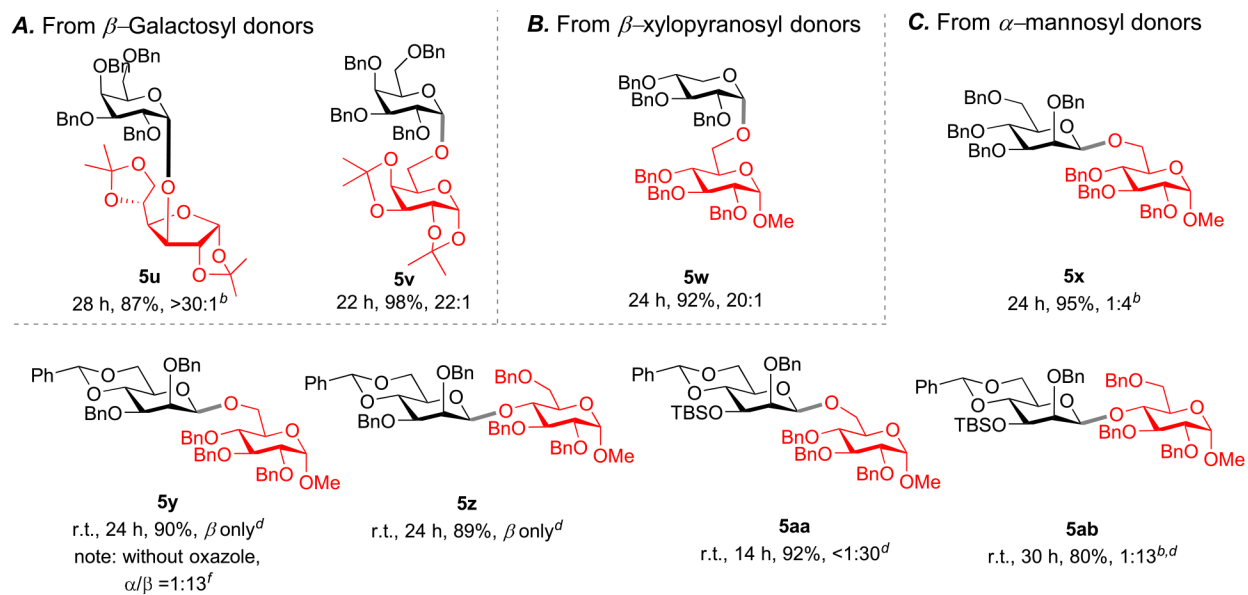


**Figure 1.**  
Strategies for stereoselective glycosylation and our design.



**Figure 2.**

Reaction scope with  $\beta$ -D-glucopyranosyl donors. <sup>a</sup>Standard condition. <sup>b</sup>Concentration: 0.02 M. Reaction was stirred at 0 °C with 12% IMesAuCl and 10% [Ag(MeCN)<sub>2</sub>]<sup>+</sup> BARF<sup>-</sup>. <sup>c</sup>Concentration: 0.08 M. DCM and cyclohexane (*v/v* = 1:1) were used as the solvent. Reaction was run at 0 °C. <sup>d</sup>Concentration: 0.04 M. Reaction was stirred at -15 °C with 12% IMesAuCl and 10% [Ag(MeCN)<sub>2</sub>]<sup>+</sup> BARF<sup>-</sup>. PhCF<sub>3</sub> and cyclohexane (*v/v* = 1:1) were used as the solvent. <sup>e</sup>Using 2.0 equiv of acceptors.

**Figure 3.**

Reaction scope with other 1,2-*trans*-monosaccharide donors. <sup>a</sup>Standard conditions. <sup>b</sup>Using 2.0 equiv of acceptors. <sup>c</sup>Reaction was run in 0.02 M PhCF<sub>3</sub>, with 1.2 equiv of acceptor, using 10% PPh<sub>3</sub>AuNTf<sub>2</sub> as catalyst and at -25 °C. <sup>d</sup>Reaction was run at room temperature. <sup>e</sup>NMR yield. <sup>f</sup>See the Supporting Information for details.

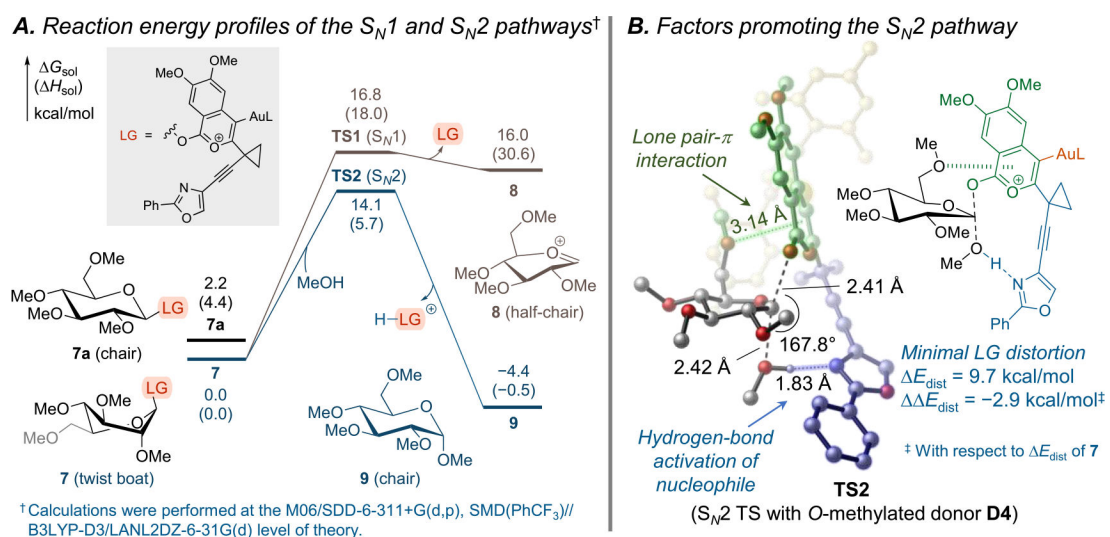
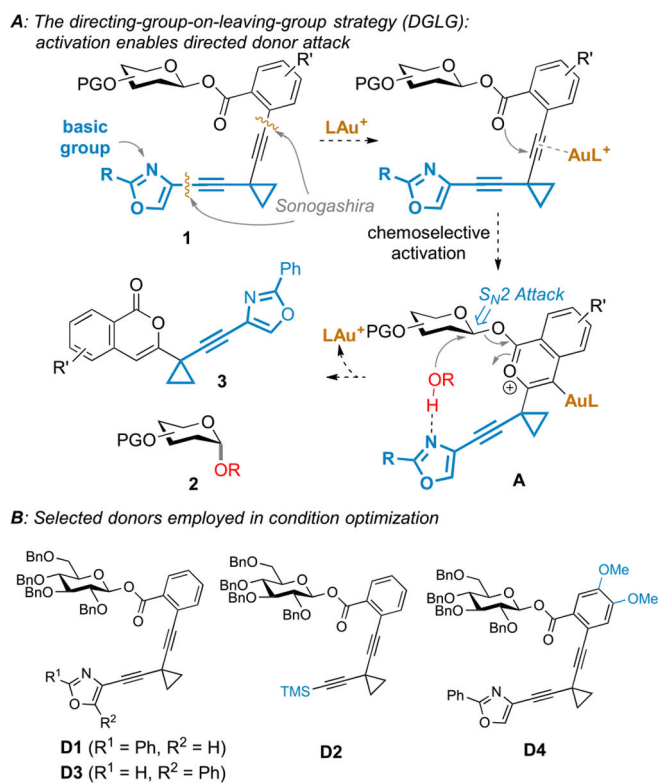
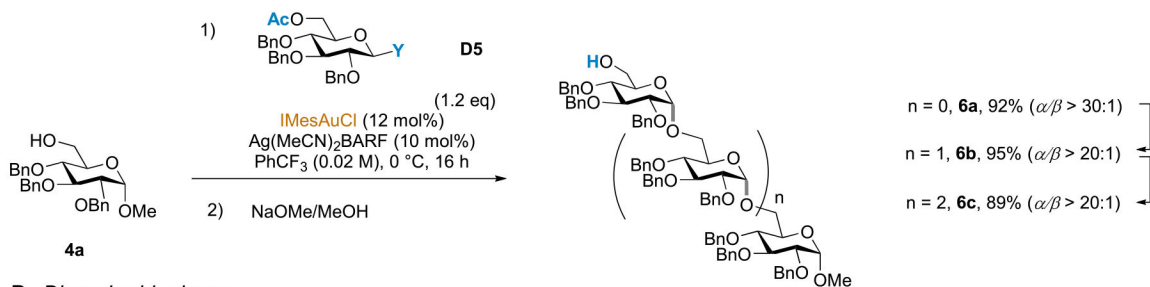


**Figure 4.**  
Computational mechanistic studies.

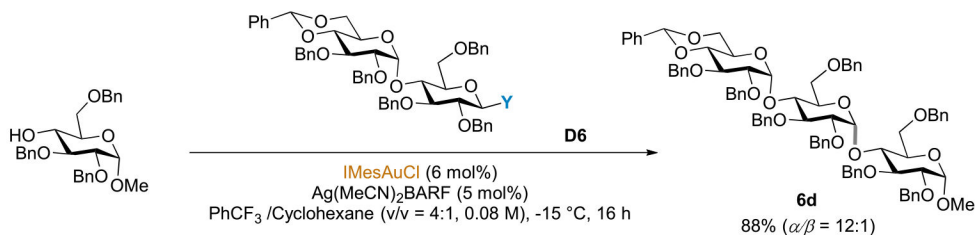


**Scheme 1. Implementing the “Traceless” Directing Group Design**

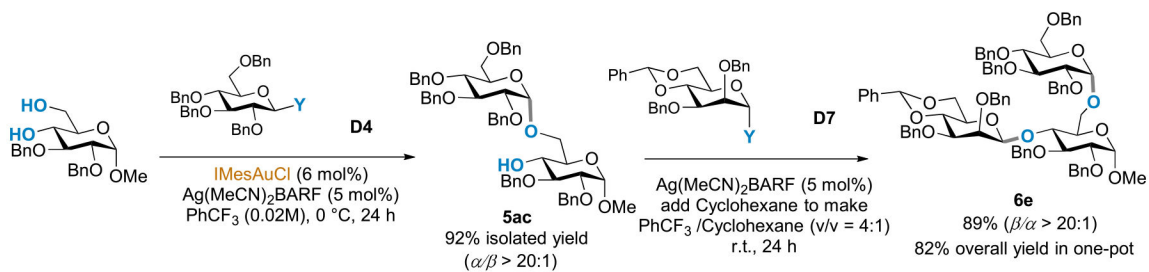
### A. Iterative synthesis of isomaltotetraose



### B. Disaccharide donor



### C. One-pot chemoselective synthesis



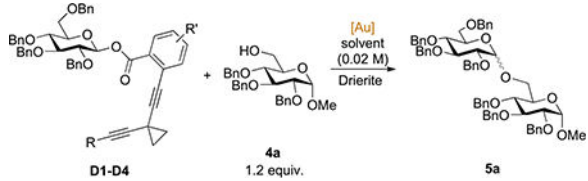
<sup>a</sup>Y = the oxazole-functionalized leaving group.

### Scheme 2. Synthesis of Oligosaccharides<sup>a</sup>

<sup>a</sup>Y = the oxazole-functionalized leaving group.

Table 1.

## Reaction Discovery and Optimization



entry	donor	catalyst (equiv) <sup>a</sup>	solvent (conc.)	temp./time	yield ( $\alpha/\beta$ ) <sup>b</sup>
1	D1	A	DCM	-35 °C/24 h	95% (11:1)
2	D2	A	DCM	-35 °C/24 h	95% (1.5:1)
3	D1	A <sup>c</sup>	DCM	-35 °C/12 h	95% (2.8:1)
4	D1	A <sup>d</sup>	DCM	-35 °C/12 h	96% (1.5:1)
5	D3	A	DCM	-35 °C/24 h	<5% (N/A) <sup>e</sup>
6	D4	A	DCM	-35 °C/5 h	96% (11:1)
7	D4	B	DCM	0 °C/16 h	62% (>20:1) <sup>e</sup>
8	D4	B	PhCF <sub>3</sub>	0 °C/16 h	>99% (>20:1)
9	D4	B	PhCF <sub>3</sub>	-15 °C/24 h	41% (30:1) <sup>e</sup>
10	D4	B	<i>f</i>	-15 °C/15 h	>99% <sup>g</sup> (27:1)
11	D2	B	<i>f</i>	-15 °C/10 h	92% <sup>h</sup> (3.1:1)

<sup>a</sup>A: Ph<sub>3</sub>PAuNTf<sub>2</sub> (20 mol %); B: IMesAuCl (6 mol %)/[Ag-(MeCN)<sub>2</sub>]<sup>+</sup> BARF<sup>-</sup> (5 mol %).

<sup>b</sup>Combined NMR yield and anomeric ratio determined by NMR.

<sup>c</sup>Using 50 mol % catalyst instead.

<sup>d</sup>Using 1 equiv of catalyst instead.

<sup>e</sup>Conversion is nearly the same as yield.

<sup>f</sup>PhCF<sub>3</sub> and cyclohexane (*v/v* = 4:1) were used as the solvent and the initial substrate concentration is 0.08 M.

<sup>g</sup>97% isolated yield.

<sup>h</sup>93% conversion.